JOURNAL OF PROPULSION AND POWER
Vol. 25, No. 5, September–October 2009

Mitigation of Graphite Nozzle Erosion by Boundary-Layer Control in Solid Rocket Motors

Piyush Thakre* and Vigor Yang†
Pennsylvania State University, University Park, Pennsylvania 16802

DOI: 10.2514/1.41293

A comprehensive analysis is performed to study the mitigation of graphite nozzle erosion in solid rocket motors loaded with nonmetallized ammonium perchlorate/hydroxyl-terminated polybutadiene composite propellants. The work extends our earlier model for predicting the chemical erosion of nozzle materials to include a nozzle boundary-layer control system. The strategy involves injection of relatively low-temperature species, obtained from reactions of an ablative material (succinic acid/polyvinyl acetate) and a small amount of propellant combustion gases, to a location slightly upstream of the nozzle throat. The formulation takes into account the detailed thermofluid dynamics of a multicomponent reacting flow, heterogeneous reactions at the nozzle surface, and condensed-phase energy transport. The effect of nozzle boundary-layer control system injection on the near-surface physiochemistry is investigated. Various fundamental mechanisms dictating the effectiveness of the nozzle boundary-layer control system are identified and quantified. The calculated erosion rates with the nozzle boundary-layer control system are negligible for the vertical injection, even at ultrahigh pressures. The mitigation of nozzle erosion is attributed primarily to the low temperature of the injected fluid, and secondarily to the reduced concentrations of oxidizing species, H_2O, CO_2, and OH, near the nozzle surface. A parametric study is also conducted to determine the influence of such nozzle boundary-layer control system operating parameters as temperature, velocity, and injection angle.

Nomenclature

A_i	=	preexponential factor for rate constant in reaction i
b_i	=	temperature exponent for rate constant in reaction i
E_i	=	activation energy for reaction i
$\dot{m}$	=	mass flow rate
p	=	pressure
p_t	=	chamber pressure
R	=	particular gas constant
Re	=	Reynolds number
R_u	=	universal gas constant
r	=	radial coordinate
T	=	temperature
T_{inj}	=	injection temperature
T_t	=	chamber temperature
$u_{r\text{-inj}}$	=	nozzle boundary-layer control system injection velocity
x	=	axial coordinate
Y_i	=	mass fraction of species k
θ_{inj}	=	angle of nozzle boundary-layer control system injection
$\dot{\omega}$	=	species mass production rate

Subscripts

div	=	diverted
inj	=	injection
pyro	=	pyrolysis
s	=	surface

I. Introduction

THE erosion of a rocket-nozzle throat during motor operation leads to several problems. The material erosion reduces the area ratio of the nozzle exit to the throat, and consequently decreases the propulsive efficiency of the vehicle. The nozzle surface recession rate should be accounted to accurately predict the performance of a rocket motor. Graphite and carbon–carbon composites, which are widely used as nozzle materials, undergo significant erosion at high chamber pressures and temperatures [1–3]. The surface recession is primarily due to the chemical erosion caused by heterogeneous reactions between the nozzle material and oxygen-containing species (e.g., H_2O, OH, and CO_2) in the propellant combustion products. Several comprehensive models [4–6] have been established to predict the nozzle erosion in practical rocket-motor environments. The erosion rate was found to increase linearly with the chamber pressure. Because a throat-area increase of more than 5% is considered alarming for most propulsion applications, the erosion level for ultrahigh pressures ($\sim$50 MPa) and long-duration firings can become unacceptable. It is thus crucial to devise methods to mitigate nozzle throat erosion over a wide range of operating conditions, especially at high pressures.

One approach to reducing erosion is to develop propellants that yield minimal concentrations of undesirable oxidizing species. This may, however, not be practical from the perspective of system implementation in the near term. It is known that the chemical erosion of a nozzle can also be lowered by increasing the aluminum (Al) content in a metallized ammonium perchlorate/hydroxyl-terminated polybutadiene (AP/HTPB) propellant [2]. But the resultant increase in alumina slag ($Al_2O_{3(l)}$) may reduce the delivered performance of the motor, due to thermal and momentum-lag losses associated with two-phase flow. The overall combustion efficiency may also decrease, leading to some unburnt Al. In addition, there would be an increase in mechanical erosion due to impingement of condensed-phase Al_2O_3 particulates on the nozzle surface, especially for submerged nozzles. Refractory metals such as tungsten, rhenium, molybdenum, and their alloys have been used as materials for nozzle inserts, because they can resist chemical erosion more effectively than carbon-based materials [6,7]. Unfortunately, the cost and weight penalties associated with these metals may sometimes render their use uneconomical. Refractory ceramic materials have also been employed, due to their remarkable erosion resistance. Although ceramics present lesser weight penalties than refractory metals, they are known to

Received 28 September 2008; accepted for publication 6 June 2009.

*Ph.D. Candidate, Department of Mechanical and Nuclear Engineering; pkt109@psu.edu.

†John L. and Genevieve H. McCain Chair in Engineering, Department of Mechanical and Nuclear Engineering; currently Georgia Institute of Technology; vigor.yang@aerospace.gatech.edu. Fellow AIAA.

frequently suffer from cracking caused by thermal shocks [7]. Much effort has been made to address this issue by developing new materials. A notable example is composites of zirconium carbide (ZrC) and tungsten, which exhibit a strong resistance to both erosion and thermal shocks [8].

Nozzle erosion can possibly be reduced by modifying the nozzle geometry. The extent of reduction, however, may be too small to dedicate efforts in this direction. For nonmetallized propellants, the Bartz correlation [9] suggests that the rate of heat transfer to the nozzle surface is inversely proportional to the diameter. Because nozzle erosion is directly correlated with heat transfer, a decrease in the throat diameter may possibly decrease the erosion rate. In practice, the nozzle diameter is selected based on other motor-operating parameters, and it may not be desirable to change the diameter solely from the perspective of erosion mitigation. It has been reported that a relatively long cylindrical throat section helps reduce erosion [10]. This phenomenon is attributed to the fact that a longer subsonic entry length leads to a thicker boundary layer, thereby decreasing the erosion rate. Such a long nozzle increases the weight penalty and consequently nullifies the advantage of reduced erosion.

In addition to the implementation of erosion-resistant materials, the problem can be circumvented by exercising some sort of control on the nozzle boundary layer. Because the temperature and oxidizing-species concentrations near the surface are the two key parameters dictating chemical erosion [5], any effective scheme for minimizing erosion must be executed through these parameters. Wolt and Webber [11] appear to have been the first to employ the so-called nozzle boundary-layer control system (NBLCS). Figure 1a shows a schematic of the NBLCS configuration for a solid rocket motor. The system diverts a small portion ($\dot{m}_{\mathrm{div}}$) of hot combustion product gases from the chamber, and allows it to pass over grains of such ablative materials as succinic acid (SA) and polyvinyl acetate (PVA), as shown in a close-up view in Fig. 1b. The species generated from the interaction between the diverted propellant combustion products and the ablative material are injected slightly upstream of the nozzle throat, with a temperature much lower than the flame temperature of the solid propellant. Furthermore, the mass fractions of oxidizing species H_2O, CO_2, and OH near the nozzle surface are substantially reduced as compared with those in the propellant combustion product stream.

Direct film cooling by injecting an inert, low-temperature fluid is not practical for solid rockets due to the performance degradation and weight/volume penalty. The NBLCS approach appears to be more practical and feasible from the technology implementation point of view. It is much better to use whatever is available on board and then carry a small mass of ablative solid grains. The purpose of the present work is to conduct a comprehensive theoretical/numerical study on the mitigation of nozzle throat erosion by employing the NBLCS. The analysis simulates the experimental study reported in [12]. Special attention is given to the effect of the injected flow on the physiochemical processes near the nozzle surface. In addition, a parametric study of the dependence of nozzle erosion on the NBLCS injection temperature, velocity, and geometric orientation is carried out to optimize the system effectiveness.

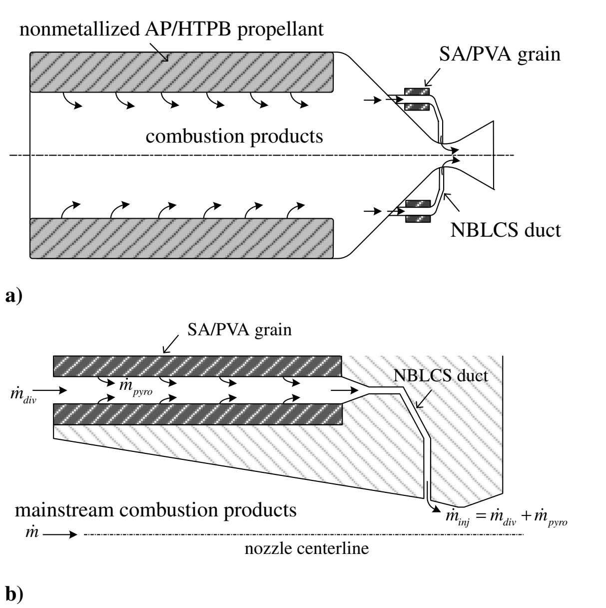

Fig. 1 Shown are the following: a) schematic of solid rocket motor with nozzle boundary-layer control system, and b) close-up view of NBLCS duct and injection location. Concept adopted from [17,19].

II. Theoretical Formulation and Numerical Methods

Figure 2a shows the physical domain of concern, including a graphite nozzle and an NBLCS injection for erosion mitigation. The flow entering the nozzle consists of the combustion products of a nonmetallized AP/HTPB propellant. The main species considered are H_2O, CO_2, CO, HCl, N_2, H_2, OH, and H. Minor species, NO, O_2, and O, are ignored, as they are present in negligible concentrations due to the fuel-rich nature of the propellant. The basis of the present analysis is the general framework developed and validated in our previous study of graphite nozzle erosion [5]. The formulation involves general conservation equations for the gas phase, energy transport in the solid phase, interfacial conditions between the gas and the solid phases, and the outer boundary condition of the nozzle material. The gas-phase dynamics are modeled using the Favre-averaged conservation equations of mass, momentum, energy, and species concentration in axisymmetric coordinates. Turbulence closure is achieved by means of a well-calibrated two-layer turbulence model suitable for transpiration and accelerating flows [5,13]. Full account is taken of variable transport and thermodynamic properties. Table 1 summarizes the kinetics data employed for the heterogeneous reactions at the graphite nozzle surface.

The governing equations and associated boundary conditions are solved numerically by means of a density-based finite volume approach with body-fitted coordinates. The methodology adopted for turbulence modeling, time integration, and spatial discretization is detailed in [5]. The code has been implemented on a parallel computing facility by employing a distributed-memory message passing interconnection. The grid is stretched in the radial direction and clustered near the wall, to resolve the near-surface flowfield with high fidelity. The centers of the computational cells adjacent to the nozzle surface are located at $y^+ < 1$, to accurately capture the near-wall phenomena. The current study predicts the erosion rate at steady state attained within a second of motor operation. Because the erosion rate is on the order of one-tenth of mm/s, the change in the nozzle geometry is not significant for the time duration of interest. Consequently, a moving wall boundary was not considered.

III. Nozzle Configuration with Nozzle Boundary-Layer Control System and Boundary Conditions

The nozzle and the NBLCS injection configuration are shown in Fig. 2b. The injection is vertical ($\theta_{\mathrm{inj}} = 90$ deg) and axisymmetric, with the port width being 0.15 cm. The pressure (p_t) and temperature

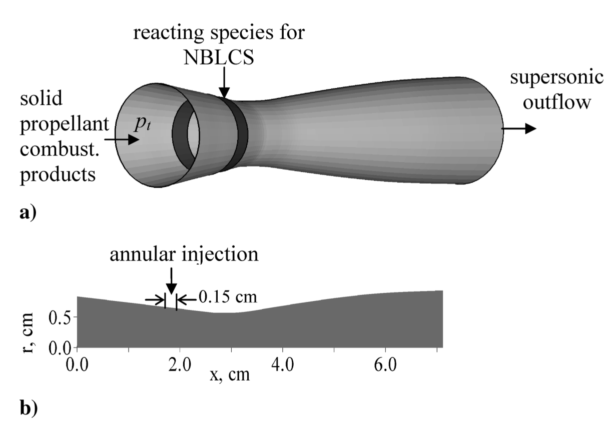

Fig. 2 Rocket nozzle with flow injection from nozzle boundary-layer control system.

Table 1 Kinetic data[a] for heterogeneous reactions at the graphite nozzle surface [14,15]

Surface reaction	A_i	B	E_i, kcal/mol	$\dot{\omega}_i$, kg/m^2/s
$C_{(s)} + H_2O \rightarrow CO + H_2$	4.8×10^5 kg/(m$^2 \cdot$ s $\cdot$ atm$^{0.5}$)	0.0	68.8	$k_i p_{H_2O}^{0.5}$
$C_{(s)} + CO_2 \rightarrow 2CO$	9.0×10^3 kg/(m$^2 \cdot$ s $\cdot$ atm$^{0.5}$)	0.0	68.1	$k_i p_{CO_2}^{0.5}$
$C_{(s)} + OH \rightarrow CO + H$	3.61×10^2 kg $\cdot$ K$^{0.5}$/(m$^2 \cdot$ s $\cdot$ atm)	−0.5	0.00	$k_i p_{OH}$

[a]$k_i = A_i T_s^b \exp(-E_i/R_u T_s)$, the rate of graphite consumption is obtained in kg/m^2/s.

(T_t) at the nozzle inlet are specified according to the chamber conditions. The velocity at the exit is supersonic. Table 2 lists the species mass fractions at the nozzle inlet obtained from the chemical equilibrium calculation [16] for a nonmetallized AP/HTPB propellant at $p_t = 6.9$ MPa. Three different chamber pressures and their corresponding flame temperatures are used to study the effect of motor-operating conditions and the NBLCS on the nozzle erosion. The species mass fractions remain nearly constant in the pressure range of 6.9–45 MPa. The ambient temperature is taken as 300 K.

In the experimental study conducted by Evans et al. [3,12] to implement the NBLCS in a rocket-motor simulator, a small portion of propellant combustion gases from the combustion chamber is diverted and passed over multiple center-perforated grains of the ablative material made of SA/PVA (90/10 by mass). This material has a relatively low pyrolysis temperature. The energy transfer from the diverted combustion gases pyrolyzes the SA/PVA grain. The species resulting from the reactions between the diverted propellant combustion gases ($\dot{m}_{\mathrm{div}}$, about 1% of the total mass flow rate) and pyrolyzed SA/PVA ($\dot{m}_{\mathrm{pyro}}$) are introduced slightly upstream of the nozzle throat through four injection ports. The fuel-rich species so formed can serve as scavengers for the oxidizing species in the boundary layer. The injection mass flux ($\dot{m}_{\mathrm{inj}}$) through each of the four injection ports is given by

$$\dot{m}_{\mathrm{inj}} = \dot{m}_{\mathrm{div}} + \dot{m}_{\mathrm{pyro}} \tag{1}$$

Kuo et al. [17] experimentally characterized the pyrolysis of SA/PVA grains in the temperature range of 543–1163 K, by employing a confined rapid thermolysis technique as well as a conduction-driven heat transfer. It was found that the SA/PVA grain, when subject to rapid heating, melts and/or evaporates without undergoing any decomposition. A linear regression rate of the grain was established as a function of heat flux. A companion study of the flow through the NBLCS injection port was conducted by Acharya and Kuo [18,19]. Their calculations suggest that the ratio of $\dot{m}_{\mathrm{div}}$ to $\dot{m}_{\mathrm{pyro}}$ falls in the range of 0.2–0.3, after a steady-state motor-operating condition is attained. In practice, however, the value of $\dot{m}_{\mathrm{pyro}}$ continues to increase with time, due to increasing surface area of the cylindrical SA/PVA grain during pyrolysis. Because the high heat flux from the diverted propellant combustion gases leads to rapid pyrolysis of SA/PVA, it is reasonable to assume an equilibrium composition at the NBLCS exit [17,19]. The local temperature varies between 1000 and 1500 K [16], depending on the value of $\dot{m}_{\mathrm{div}}/\dot{m}_{\mathrm{pyro}}$.

Table 2 Rocket-nozzle inlet flow conditions[a]

Combustion product species (nonmetallized AP/HTPB propellant)	
Y_{H_2O}	0.29
Y_{CO_2}	0.22
Y_{CO}	0.11
Y_{H_2}	0.003
Y_{OH}	0.01
Y_H	0.00
Y_{N_2}	0.10
Y_{HCL}	0.267
Motor-operating conditions	
p_t, MPa	6.9, 15, 45
T_t, K	3000, 3040, 3065
T_{amb}, K	300

[a]Nozzle material density = 1.92 g/cc, throat radius = 0.57 cm, average thickness = 4.8 cm.

In the current analysis, the value of $\dot{m}_{\mathrm{div}}/\dot{m}_{\mathrm{pyro}}$ was taken to be constant at 0.3. Two different injection temperatures (T_{inj}) of 1200 and 1500 K were considered. The injection velocity ($u_{r\text{-inj}}$) was estimated to be in the range of 100–120 m/s, according to mass conservation. It should be noted that the values of $\dot{m}_{\mathrm{div}}/\dot{m}_{\mathrm{pyro}}$, T_{inj}, and $u_{r\text{-inj}}$ used here are only representative values that are likely to exist at the injection location. The estimates are believed to be sufficiently accurate for the purpose of evaluating the ability of the NBLCS to reduce nozzle throat erosion. The actual values may be somewhat different and may vary marginally with time during the course of motor operation. Although the injection has been treated as axisymmetric, in practice, there would be some three-dimensional effects due to the nonuniformity of injected flow. The species mass fractions at the injection port were calculated through the chemical equilibrium analysis [16]. Table 3 lists the inlet conditions at the NBLCS injection port. The concentrations of the oxidizing species of H_2O and CO_2 are reduced significantly, as compared with their counterparts at the nozzle entrance. OH radical was not considered at the injection port, due to its negligible concentration.

IV. Results and Discussions

The theoretical/numerical framework described in the preceding sections was implemented to explore the effect of NBLCS on the chemical erosion of graphite nozzles in practical rocket-motor environments. Only the upper half of the nozzle is simulated due to flow symmetry. The axisymmetric computational domain in Fig. 2 is divided into 141×80 grid points in the x and r directions, respectively. The NBLCS injection temperature is 1200 K unless mentioned otherwise. The turbulent flow development in the same nozzle configuration was detailed earlier [5]. The gas-phase reactions were not considered in our previous studies because of their negligible effect on nozzle erosion [5]. In the present case, chemical reactions among the AP/HTPB combustion products and the injected species may occur in the boundary layer. Such reactions, however, will not have any significant impact on either the concentrations of H_2O, OH, and CO_2 or the rate of heat transfer to the nozzle wall.

Two types of calculations for NBLCS, with and without surface reactions, were conducted. The results were systematically compared with the case without any NBLCS injection, to highlight the impact of this strategy. First, calculations were performed without including any heterogeneous surface reaction along the nozzle wall. The adiabatic wall condition was also enforced. The purpose was to examine the effect of NBLCS injection on the development of the flow and concentration fields, especially in the near-surface region. The results also provided a basis for clearly identifying the impact of surface reactions on the nozzle flow evolution. Figure 3a shows the distribution of the vertical velocity component in the nozzle interior. As expected, the vertical velocity is quite high at the injection

Table 3 Flow conditions at NBLCS injection port

Species	Mass fractions
Y_{H_2O}	0.06
Y_{CO_2}	0.03
Y_{CO}	0.76
Y_{H_2}	0.05
Y_{N_2}	0.03
Y_{HCL}	0.07
T_{inj}, K	1500, 1200
$u_{r\text{-inj}}$, m/s	100

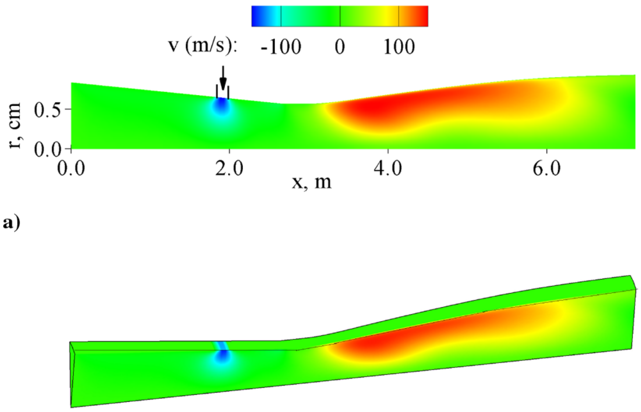

Fig. 3 Two views showing distribution of vertical velocity in nozzle interior ($T_t = 3000$ K, $p_t = 6.9$ MPa, $T_{\mathrm{inj}} = 1200$ K, no surface reactions, adiabatic wall).

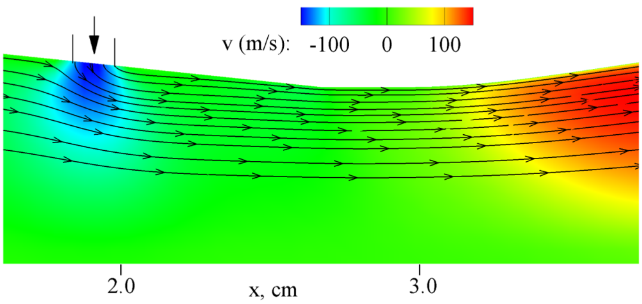

Fig. 4 Close-up view of stream traces near NBLCS injection and nozzle throat ($T_t = 3000$ K, $p_t = 6.9$ MPa, $T_{\mathrm{inj}} = 1200$ K, no surface reactions, adiabatic wall).

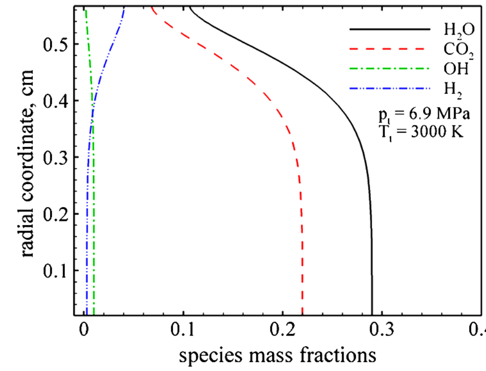

Fig. 6 Radial distributions of species at nozzle throat ($x = 2.65$ cm) with NBLCS injection ($T_t = 3000$ K, $p_t = 6.9$ MPa, $T_{\mathrm{inj}} = 1200$ K, no surface reactions, adiabatic wall).

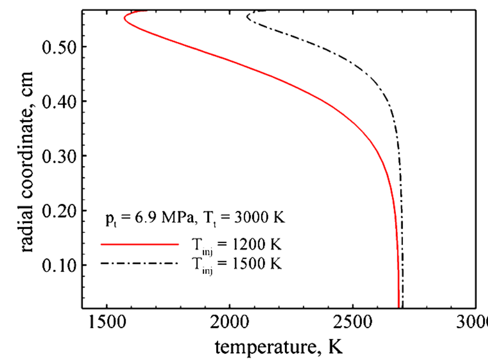

Fig. 7 Radial distributions temperature at nozzle throat ($x = 2.65$ cm) with NBLCS injection ($T_t = 3000$ K, $p_t = 6.9$ MPa, no surface reactions, adiabatic wall).

location, reaching a local maximum value of about 120 m/s. The velocity increases downstream of the throat, due to the flow expansion caused by the divergent geometry. Figure 3b shows a tilted view of the vertical velocity distribution, highlighting the strategy of axisymmetric injection for mitigating erosion in a circumferentially uniform manner. Figure 4 presents a close-up view of the flowfield and associated streamlines near the injection port. The incoming flow from the combustion chamber is pushed slightly downward. The injection exerts limited influence on the bulk of the nozzle flow. Consequently, the nozzle efficiency and overall vehicle thrust remain almost unaffected. The nozzle throat regime is basically covered by the flow originating from the NBLCS injection port. Figure 5 shows the distributions of temperature and mass fractions of H_2O, CO_2, and OH. The injection of fuel-rich species gives rise to a concentration boundary layer above the nozzle surface. The effect is present even slightly upstream of the injection port because of species diffusion. Both the temperature and oxidizing-species concentrations decrease substantially in the near-surface region.

The effect of the NBLCS injection on the radial distributions of the oxidizing-species concentrations and temperature was studied. Figure 6 shows the result at the nozzle throat ($x = 2.65$ cm). The mass fraction of H_2O drops from 0.29 at the centerline to 0.114 at the surface. The corresponding values for CO_2 are 0.22 and 0.0074, respectively. The OH mass fraction at the throat is negligible. On the other hand, the mass fraction of H_2 at the throat increases from 0.003 at the centerline to 0.039 at the surface. Figure 7 shows the radial distributions of temperature at the throat for two different injection temperatures of 1200 and 1500 K. The temperature drops from about 2600 K at the centerline to 1670 K at the surface for the former case and to 2150 K for the latter case. The temperature profiles do not decrease monotonically from the centerline. The rise near the surface results from the dissipation of the flow kinetic energy into its thermal

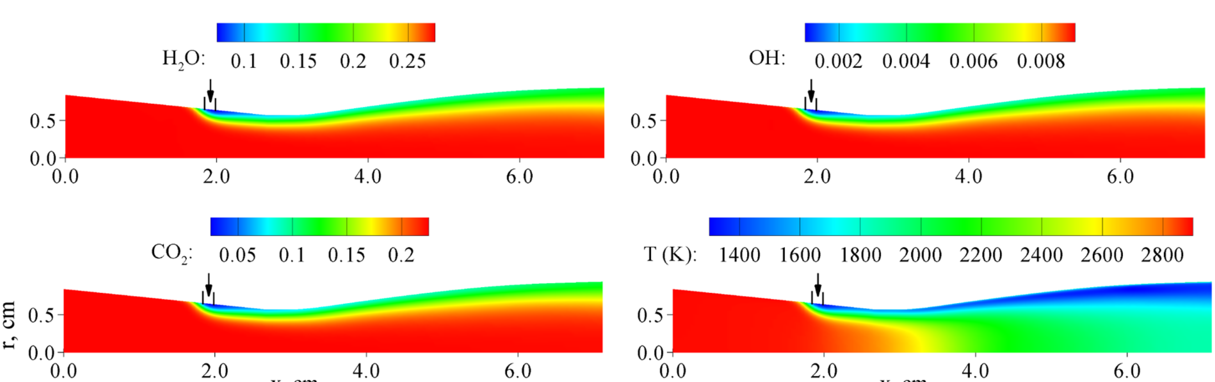

Fig. 5 Distribution of mass fraction of H_2O, CO_2, and OH and temperature in nozzle interior ($T_t = 3000$ K, $p_t = 6.9$ MPa, $T_{\mathrm{inj}} = 1200$ K, no surface reactions, adiabatic wall).

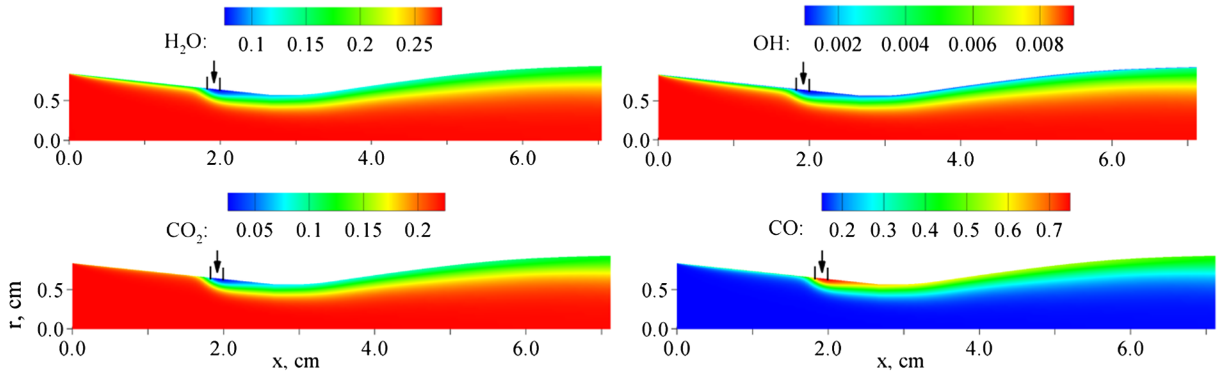

Fig. 8 Distribution of mass fraction of H_2O, CO_2, OH, and CO in nozzle interior ($T_t = 3000$ K, $p_t = 6.9$ MPa, $T_{\mathrm{inj}} = 1200$ K, surface reactions, conductive wall).

energy. The reduction in the near-surface temperature and oxidizing-species concentrations, as compared with their counterparts in the noninjection case, augurs well for minimizing the nozzle erosion.

To study the chemical erosion of the graphite nozzle material, the three heterogeneous surface reactions summarized in Table 1 were implemented. The oxidizing species of CO_2, H_2O, and OH are consumed at the surface to form CO, H_2, and H. The temperature boundary condition at the nozzle surface is made conductive by considering the energy transport in the solid phase [5]. Figure 8 shows the distributions of mass fractions of H_2O, CO_2, OH, and CO for the case with surface reactions and a conductive nozzle wall. Unlike the situation shown in Fig. 5 without surface reactions, the species concentration gradients exist from the nozzle entrance, due to the combined effect of surface reactions and the NBLCS injection. Figures 9 and 10 show, respectively, the radial distributions of mass fractions of H_2O and CO_2 at the nozzle throat. Both cases with and without the NBLCS are included. As expected, the injection of boundary-layer control gases reduces the H_2O and CO_2 concentrations at the surface. The value of H_2O mass fraction at the surface ($\sim$0.107) is very close to that ($\sim$0.114) shown in Fig. 6, where surface reactions were turned off. A limited quantity of H_2O is consumed at the surface, which indicates that minimal chemical erosion takes place when the NBLCS is activated. A similar comparison of CO_2 mass fractions was made between Figs. 6 and 10. Almost no CO_2 is consumed in the NBLCS case. The rate of graphite consumption by CO_2 is rendered negligible because of the drop in the nozzle surface temperature.

Figure 11 shows the distributions of temperature in the nozzle interior under conditions with and without the NBLCS injection. The NBLCS proves very effective in lowering the nozzle surface temperature downstream of the injection port. Figure 12 shows the radial distributions of temperature at the throat for injection temperatures of 1200 and 1500 K. The surface temperatures reduce to 1640 and 2015 K, respectively, as compared with 2285 K for the noninjection case. The value of 1640 K is slightly lower than its counterpart of 1670 K in Fig. 7, on account of the endothermicity of the surface reactions and wall heat transfer. The small difference in the surface temperature, however, indicates very nominal rates of surface reactions in the NBLCS case. Figure 13 shows the axial distribution of the surface temperature along the entire length of the nozzle. The surface temperatures are identical for all of the three cases upstream of the injection port. The NBLCS injection results in a sharp decrease near the injection port and in its downstream region.

Figure 14 shows the distribution of the graphite erosion rate along the entire length of the nozzle, for the cases with and without the NBLCS injection. The erosion rates at the nozzle inlet start at nearly the same level for all cases, but the rate drops significantly for the NBLCS cases in the region downstream of the injection port. The calculated erosion rate at the throat with NBLCS injection is much lower (0.027 mm/s for $T_{\mathrm{inj}} = 1500$ K and 0.0033 mm/s for $T_{\mathrm{inj}} = 1200$ K) than for the noninjection case (0.124 mm/s). The erosion is found to be negligible when the injection temperature falls below 1200 K. Figure 15 shows a comparison of graphite erosion rates at the nozzle throat at various chamber pressures under conditions with and without NBLCS. Even at high pressures, the erosion rates are negligible with the NBLCS injection. Although the species concentrations employed at the NBLCS injection port were identical for the two injection cases, the erosion rate for $T_{\mathrm{inj}} = 1200$ K was much lower than that for $T_{\mathrm{inj}} = 1500$ K. The reduction in the erosion rate is thus attributed primarily to the low injection temperature and secondarily to the reduced concentrations of oxidizing species, H_2O, CO_2, and OH, in the near-surface region. Near-zero throat erosion was also observed experimentally by Evans et al. [12] when NBLCS injection was activated.

Although the strategy of NBLCS injection shows potential to mitigate nozzle erosion, there may still be some outstanding issues with respect to its implementation on a practical rocket motor. The influence of NBLCS injection on the nozzle efficiency and overall vehicle specific impulse has to be studied in detail. The injection flow parameters must be known precisely to enable accurate predictions of

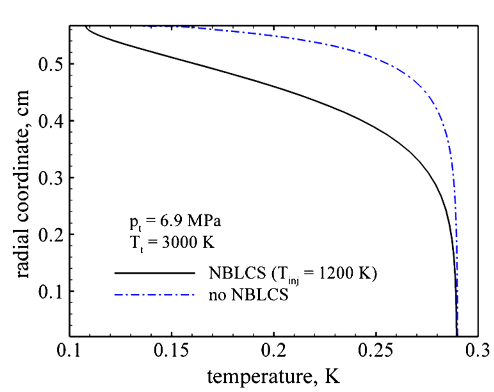

Fig. 9 Radial distributions of H_2O at nozzle throat ($x = 2.65$ cm) with and without NBLCS injection ($T_t = 3000$ K, $p_t = 6.9$ MPa, $T_{\mathrm{inj}} = 1200$ K, surface reactions, conductive wall).

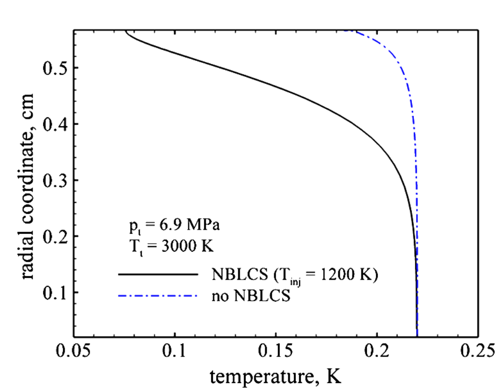

Fig. 10 Radial distributions of CO_2 at nozzle throat ($x = 2.65$ cm) with and without NBLCS injection ($T_t = 3000$ K, $p_t = 6.9$ MPa, $T_{\mathrm{inj}} = 1200$ K, surface reactions, conductive wall).

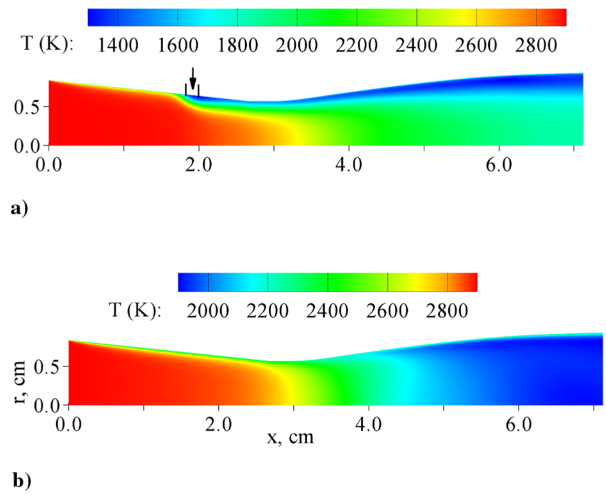

Fig. 11 Distribution of temperature in nozzle interior: a) with injection, and b) without injection ($T_t = 3000$ K, $p_t = 6.9$ MPa, $T_{\mathrm{inj}} = 1200$ K, surface reactions, conductive wall).

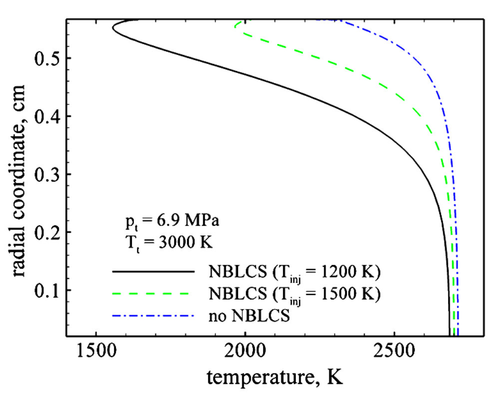

Fig. 12 Radial distributions temperature at nozzle throat with and without NBLCS injection ($T_t = 3000$ K, $p_t = 6.9$ MPa, surface reactions, conductive wall).

the nozzle erosion rate. The high-velocity vertical injection may possibly interfere with the nozzle core flow and reduce the vehicle specific impulse. Further studies are needed to find an optimum injection angle to limit the impact of NBLCS to the near-surface region. It is also necessary to ensure that the injection port does not clog during the course of motor operation. This aspect is crucial in the case of metallized propellants, where the molten alumina can condense and cover the port, thus rendering the strategy of NBLCS ineffective. The possibility of flow reversal from the nozzle interior toward the injection port must be completely eliminated. In practice,

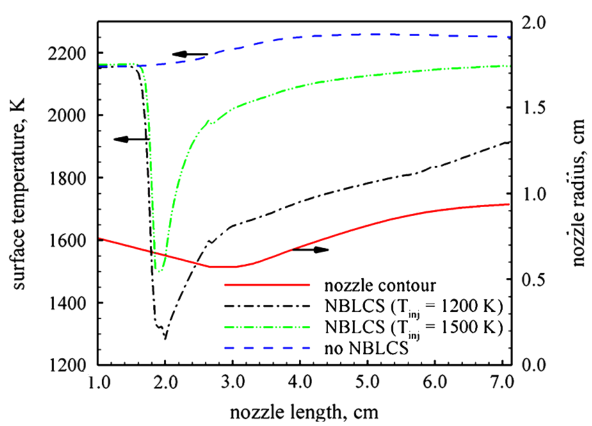

Fig. 13 Axial distributions of nozzle surface temperature with and without NBLCS injection ($T_t = 3000$ K, $p_t = 6.9$ MPa, surface reactions, conductive wall).

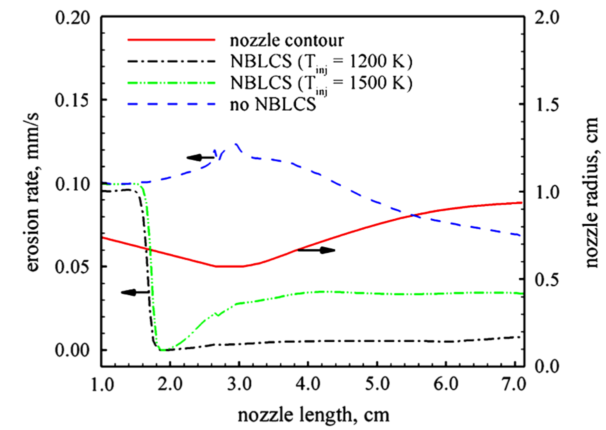

Fig. 14 Graphite nozzle erosion-rate profile with and without NBLCS injection ($T_t = 3000$ K, $p_t = 6.9$ MPa, surface reactions, conductive wall).

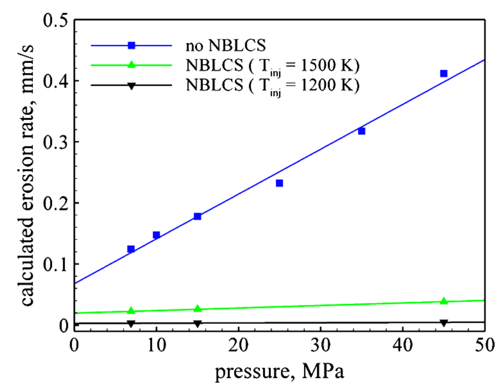

Fig. 15 Effect of chamber pressure on graphite erosion rate at nozzle throat with and without using NBLCS.

the nonuniformity of injection flow might cause some three-dimensional effects, leading to slight thrust vector misalignment issues in motors.

A parametric study of the NBLCS injection angle, velocity, and port diameter is conducted to help optimize the system design, so that throat erosion can be reduced substantially with minimal perturbation to the primary nozzle flow. The injection velocity was varied from 100 to 50 m/s, with all other conditions remaining unchanged. Figure 16 shows that the erosion rate increases with decreasing injection velocity. The reduced mass flux, as a result of the lower injection velocity, leads to a relatively higher surface temperature and a thinner boundary layer. Consequently, the erosion rate increases. Figure 17 shows the result for the injection angle of 135 deg,

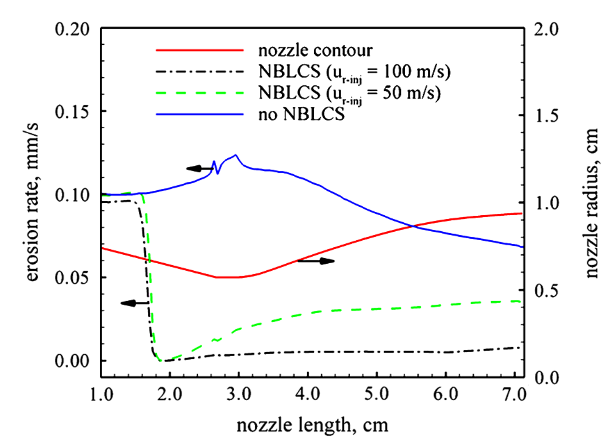

Fig. 16 Graphite nozzle erosion-rate profile with two different vertical injection velocities ($T_t = 3000$ K, $p_t = 6.9$ MPa, $T_{\mathrm{inj}} = 1200$ K).

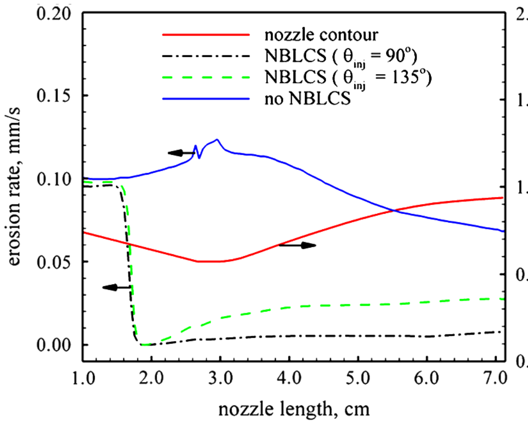

Fig. 17 Graphite nozzle erosion-rate profile with two different injection angles ($T_t = 3000$ K, $p_t = 6.9$ MPa, $T_{\mathrm{inj}} = 1200$ K, $u_{r\text{-inj}} = 100$ m/s).

measured from the positive x axis. The injection temperature and velocity remained fixed at 1200 K and 100 m/s, respectively. The erosion rate with vertical injection is lower than that for the case of $\theta_{\mathrm{inj}} = 135$ deg. Nonvertical injection leads to a thinner boundary layer, thereby causing more severe erosion.

V. Conclusions

A comprehensive theoretical/numerical analysis was performed to study the mitigation of graphite nozzle erosion in solid-propellant rocket motors by employing a NBLCS. The strategy was based on the injection of relatively low-temperature species slightly upstream of the nozzle throat, which were obtained from chemical reactions between pyrolyzed ablative material (succinic acid/polyvinyl acetate) and a small diverted portion of propellant combustion gases. The thermofluid dynamics in the nozzle were investigated in detail. Special attention was given to the flow evolution, species transport, and chemical reactions near the nozzle surface. Results indicate that the NBLCS injection had a limited influence on the bulk of the nozzle flow. The calculated erosion rates with NBLCS are negligible for vertical injection, even at ultrahigh pressures. The mitigation of nozzle erosion is attributed primarily to the low temperature of the injected fluid, and secondarily to the reduced concentrations of oxidizing species, H_2O, CO_2, and OH, near the nozzle surface. A parametric study was also conducted to determine the dependence of nozzle erosion on such NBLCS operating parameters as temperature, velocity, and injection angle. Lower injection velocity and nonvertical injection lead to a relatively higher surface temperature and a thinner boundary layer, subsequently causing an increase in the erosion rate. Overall, the implementation of NBLCS shows a potential to substantially reduce the chemical erosion of a rocket-nozzle throat over a wide range of motor-operating conditions.

Acknowledgments

This work is supported by the U.S. Office of Naval Research as a part of a multi-university research initiative project funded under contract N00014-04-1-0683, with Judah Goldwasser and Cliff Bedford as the contract monitors. The authors would like to thank Kenneth Kuo and Brian Evans for technical discussions.

References

[1] Swope, L. W., and Berard, M. F., "Effects of Solid-Rocket Propellant Formulations and Exhaust-Gas Chemistries on the Erosion of Graphite Nozzles," *AIAA Solid Propellant Rocket Conference*, AIAA, New York, Jan. 1964.

[2] Geisler, R. L., "The Relationship Between Solid Propellant Formulation Variables and Nozzle Recession Rates," *JANNAF Rocket Nozzle Technology Subcommittee Workshop*, 1978.

[3] Evans, B., Kuo, K. K., Ferrara, P. J., Moore, J. D., Kutzler, P., and Boyd, E., "Nozzle Throat Erosion Characterization Study Using a Solid-Propellant Rocket Motor Simulator," *43rd AIAA/ASME/SAE/ASEE Joint Propulsion Conference and Exhibit*, AIAA, Reston, VA, 8–11 July 2007.

[4] Acharya, R., and Kuo, K. K., "Effect of Pressure and Propellant Composition on Graphite Rocket Nozzle Erosion Rate," *Journal of Propulsion and Power*, Vol. 23, No. 6, 2007, pp. 1242–1254. doi:10.2514/1.24011

[5] Thakre, P., and Yang, V., "Chemical Erosion of Carbon-Carbon/ Graphite Nozzles in Solid-Propellant Rocket Motors," *Journal of Propulsion and Power*, Vol. 24, No. 4, 2008, pp. 822–833. doi:10.2514/1.34946

[6] Thakre, P., and Yang, V., "Chemical Erosion of Refractory Metal Nozzle Inserts in Solid-Propellant Rocket Motors," *Journal of Propulsion and Power*, Vol. 25, No. 1, 2009, pp. 40–50. doi:10.2514/1.37922

[7] Johnston, J. R., Signorelli, R. A., and Freche, J. C., "Performance of Rocket Nozzle Materials with Several Solid Propellants," NASA TN D-3428, 1966.

[8] Dickerson, M. B., Wurm, P. J., Schorr, J. R., Hoffman, W. P., Wapner, P. G., and Sandhage, K. H., "Near Net-Shape, Ultra-High Melting, Recession-Resistant ZrC/W-Based Rocket Nozzle Liners via the Displacive Compensation of Porosity (DCP) Method," *Journal of Material Science*, Vol. 39, No. 19, 2004, pp. 6005–6015. doi:10.1023/B:JMSC.0000041697.67626.46

[9] Bartz, D. R., "A Simple Equation for Rapid Estimation of Rocket Nozzle Convective Heat Transfer Coefficients," *Jet Propulsion*, Vol. 27, No. 1, 1957, pp. 49–50.

[10] Anon., "Solid Rocket Motor Nozzles," *NASA Space Vehicle Design Criteria Monograph*, SP-8115, NASA, 1975.

[11] Wolt, P. J., and Webber, J. A., "Demonstration of a Nozzle Boundary Layer Cooling System (NBLCS) as a Means to Mitigate Nozzle Erosion," *JANNAF 40th Combustion Subcommittee Meeting*, June 2004.

[12] Evans, B., Kuo, K. K., Ferrara, P. J., Moore, J. D., Kutzler, P., and Boyd, E., "Nozzle Erosion Characterization in a Non-Metallized Solid-Propellant Rocket Motor Simulator," *7th International Symposium on Special Topics in Chemical Propulsion (ISICP)*, Sept. 2007.

[13] Tseng, I. S., and Yang, V., "Combustion of a Double-Base Homogeneous Propellant in a Rocket Motor," *Combustion and Flame*, Vol. 96, No. 4, 1994, pp. 325–342. doi:10.1016/0010-2180(94)90102-3

[14] Chelliah, H. K., Makino, A., Kato, I., Araki, N., and Law, C. K., "Modeling of Graphite Oxidation in a Stagnant-Point Flow Field Using Detailed Homogeneous and Semiglobal Heterogeneous Mechanisms with Comparisons to Experiments," *Combustion and Flame*, Vol. 104, No. 4, 1996, pp. 469–480. doi:10.1016/0010-2180(95)00151-4

[15] Bradley, D., Dixon-Lewis, G., Habik, E. S., and Mushi, E. M., "The Oxidation of Graphite Powder in Flame Reaction Zones," *Proceedings of the Combustion Institute*, Vol. 20, No. 1, 1985, pp. 931–940.

[16] Gordon, S., and McBride, B. J., "Computer Program for Calculation of Complex Chemical Equilibrium Compositions and Applications," NASA Ref. Publ. 1311, 1994.

[17] Kuo, K. K., Acharya, R., Boyd, E., and Thynell, S. T., "Pyrolysis/ Evaporation Study of Succinic Acid/Polyvinyl Acetate for Reducing Nozzle Throat Erosion," *Journal of Propulsion and Power* (to be published).

[18] Acharya, R., and Kuo, K. K., "Graphite Rocket Nozzle Erosion Rate Reduction by Boundary Layer Control Using Ablative Materials," *45th Aerospace Sciences Meeting*, AIAA, Reston, VA, 2007.

[19] Acharya, R., and Kuo, K. K., "Graphite Rocket Nozzle Erosion Rate Reduction by Boundary-Layer Control Using Ablative Materials at High Pressures," *7th International Symposium on Special Topics in Chemical Propulsion*, Sept. 2007.

S. Son
Associate Editor